Journal of Cancer Research and Clinical Oncology (2019) 145:97–107
https://doi.org/10.1007/s00432-018-2769-3

ORIGINAL ARTICLE – CANCER RESEARCH

Combination of gold nanoparticles with low-LET irradiation: an approach to enhance DNA DSB induction in HT29 colorectal cancer stem-like cells

Mahdi Abbasian[1,2] · Azam Baharlouei[2,3] · Zahra Arab-Bafrani[1,4,6] · David A. Lightfoot[5]

Received: 20 June 2018 / Accepted: 11 October 2018 / Published online: 19 October 2018

Abstract

Purpose High-linear energy transfer (high LET) irradiation has significant cytotoxic effects on different cancerous stem-like cells (CSLCs) such as colorectal CSLCs. A review of the literature has indicated that the presence of gold nanoparticles (GNPs) enables low-LET irradiation to produce highly non-homogeneous dose distributions like high-LET irradiation. The purpose of this study was to evaluate the radioresponsiveness of HT29 colorectal CSLCs under low-LET irradiation (X-ray) and in the presence of GNPs.

Methods Radioresponsiveness was evaluated using the ϒ-H2AX foci formation assay, the clonogenic assay, the cell cycle progression assay and analyses of radiobiological parameters.

Results In the presence of GNPs, the survival fraction of HT29 CSLCs was significantly reduced and caused significant changes in the radiobiological parameters after irradiation. In addition, ϒ-H2AX assay showed that in the presence of GNPs, the persistent DNA double-strand breaks were significantly increased in irradiated HT29 CSLCs. The relative biological effectiveness value of GNPs with X-rays was about 1.6 for HT-29 CSLCs at the 10% of cell survival fraction (D_{10} level) when compared to X-rays alone.

Conclusion Therefore, the combination of GNPs with X-ray irradiation has the potential to kill HT29 CSLCs greater than the X-ray alone, and may be considered as an alternative for high-LET irradiation.

Keywords Cancer stem-like cell · Gold nanoparticle · DNA DSBs · RBE value

Introduction

Colorectal cancer is the third most common malignancy and the fourth leading cause of cancer-related mortality in the world (Gandomani et al. 2017; Khiari and Hsairi 2017; Arab-Bafrani et al. 2016). Surgical resection is the first choice for colorectal cancer treatment and radiotherapy, as a standard method, is an adjuvant treatment alongside surgery. Radiotherapy can reduce local recurrence and improve long-term outcomes, particularly for rectal cancer (Zhiyun He et al. 2009; Garza-Treviño et al. 2015; Yan et al. 2016; Liu et al. 2017). Despite all the recent developments in cancer therapy, colorectal cancer recurrence is still a crucial problem, and the reason for this phenomenon is not fully understood (Cui et al. 2011; Roy and Majumdar 2012). Many studies support the hypothesis that cancer stem-like cells (CSLCs) contribute to the recurrence of tumors (Moncharmont et al. 2012; Kahlert et al. 2017). Given the important role of colorectal CSLCs in the failure of conventional

✉ Zahra Arab-Bafrani
arabbafrani@goums.ac.ir

1 Stem Cell Research Center, Golestan University of Medical Science, Gorgān, Iran

2 Department of Biotechnology, College of Agriculture, Isfahan University of Technology, Isfahan, Iran

3 Department of Microbiology, Southern Illinois University at Carbondale, Carbondale, IL 62901, USA

4 Department of Biochemistry and Biophysics, Faculty of Medicine, Golestan University of Medical Sciences, Gorgān, Iran

5 Department of Plant, Soil and Agricultural Systems, Plant Biotechnology and Genome Core-Facility, Southern Illinois University at Carbondale, Carbondale, IL 62901, USA

6 Metabolic Disorders Research Center, Golestan University of Medical Sciences, Gorgān, Iran

radiotherapy, designing a new radiotherapeutic strategy is imperative to aid the elimination of colorectal CSLCs.

Based on previous reports, high-linear energy transfer (high LET) irradiation has various advantages (Cui et al. 2011; Held et al. 2016). These include increased relative biological effectiveness (RBE), less cell cycle dependency and induction of unrepairable double-strand breaks (DSB) compared to low-LET irradiation (X-ray energy) (Okayasu et al. 2006; Hirota et al. 2014). It has been demonstrated that high-LET irradiation increases the killing effects on the CSLCs of colorectal (Cui et al. 2011), pancreatic (Oonishi et al. 2012), glioblastoma (Hirota et al. 2014; Takahashi et al. 2014b), tongue (Takahashi et al. 2014a) and breast (Sai et al. 2015) cells. However, high-LET radiation therapy is more expensive and complex than conventional radiotherapy, thus it is generally inaccessible (Cui et al. 2011; Niemantsverdriet et al. 2012). Therefore, the use of some strategies to improve conventional radiotherapy effects, such as the application of a radiosensitizer, can be considered effective and affordable.

In the last decade, gold nanoparticles (GNPs) were used as radiosensitizers (McMahon et al. 2011a) that increase cellular absorption of radiation. Based on the recent nanodosimetry model reported by McMahon et al. (2011b), in addition to the production of relatively high-energy photo and Compton electrons, interactions among radiations and GNPs produce a shower of low-energy and small-range Auger electrons. These Auger electrons deposit their energy in the vicinity of the GNPs and cause highly inhomogeneous dose distributions on the nanoscale. A combination of extremely high absorbed doses and exceedingly small volumes are the common characteristics that can be frequently seen around particle tracks in high-LET irradiation (Jain et al. 2011). Consistent with this, our previous studies revealed an enhancement of absorbed dose in HT29 cancer cells under low-LET (9 MV X-ray) irradiation in the presence of GNPs (Saberi et al. 2016). Moreover, several studies showed that in the presence of GNPs, the number of ϒ-H2AX foci was increased in irradiated cancer cells which was due to increased DNA DSBs (Chithrani et al. 2010; Butterworth et al. 2011; Chattopadhyay et al. 2013).

Based on this evidence, it was hypothesized that the combination of GNPs and low-LET irradiation may efficaciously target CSLCs. To this end, the resistance mechanism of HT29 CSLCs to the low-LET irradiation was evaluated through radiobiological parameters, cell cycle progression, cell cycle redistribution and the number of induced DNA DSBs. In this study, the changes in those parameters were assessed in the presence of GNPs. According to the authors' knowledge, this study was the first to explore whether the combination of GNPs and X-ray irradiation could enhance radiosensitization of HT29 CSLCs and whether they may be considered an alternative to high-LET irradiation.

Methods

Cell culture

Human colorectal cell line (HT29) was purchased from the Pasteur Institute (Tehran, Iran). Cells were cultured in RPMI1640 (Gibco-Invitrogen, Karlsruhe, Germany) supplement by 10% (w/v) fetal bovine serum, (Gibco-Invitrogen) and 1% penicillin and streptomycin (Sigma-Aldrich, St. Louis, MO, USA). The cells were incubated with a humidified atmosphere at 37 °C with 5% (v/v) CO_2. The cells' medium was changed every 2 days. To isolate CSLCs with the ability to form spheroid-like structures, parental cells were subcultured in serum-free DMEM/F12 medium (SFM) on collagen type I coated plates (Col/SFM). The morphological changes of HT29 cells and formation of spheroid in Col/SFM at various time points were investigated with an inverted microscopy (Nikon TS100, Tokyo, Japan). Also, for viewing the three-dimensional conformation of HT29 spheroid on collagen-coated plate using a scanning electron microscopy (SEM), samples were prepared as previously reported (Girard et al. 2013). The GNPs, stabilized in a suspension of 0.1 mM PBS, were spherical with a 47–53-nm core and a 51–63-nm hydrodynamic diameter. The peak SPR (surface plasmon resonance) wavelength of the nanoparticles and zeta potential were 535 nm and −39 MV, respectively. The optimum concentration (lowest level of toxicity with highest rate of uptake) of the GNPs was 80 µM, as evaluated in our previous study (Saberi et al. 2016). HT29 CSLCs and parental cells were incubated with a final concentration of 80 µM GNPs (Sigma-Aldrich, St. Louis, MO, USA), 24 h before irradiation.

Evaluation of stemness parameters

Flow cytometry

CD133 expression was assessed in single cell suspensions of HT29 CSLCs and parental cells. Briefly, the cells were washed twice with PBS and suspended in the sample buffer [PBS, 0.5% (w/v) BSA and 2 mM EDTA]. The samples were mixed and incubated in the dark for 30 min at 40 °C after adding FCR blocking reagent and anti-CD133 (CD133/PE Human monoclonal, Miltenyi Biotech). The analysis was performed with FACS caliber (BD Biosciences, USA) using the Cell Quest software.

Quantitative real-time, reverse transcription PCR (qRT-PCR)

Relative gene expression was analyzed using qRT-PCR. Total RNA was extracted from HT29 CSLCs and parental cells using GeneAll RiboEx kit (GeneAll Biotechnology, Seoul, Korea) according to the manufacturer's protocol. Complementary DNA (cDNA) was synthesized using the SuperScript II reverse transcriptase (Invitrogen, Carlsbad, CA, USA). qRT-PCR was performed with an ABI PRISM 7300 instrument (Applied Biosystems, Foster, US) using SYBR Green PCR Core Reagents (Thermo Scientific). The primers are shown in Table 1. Standard curves were drawn using serial dilutions of pooled cDNA, including seven dilutions from 1/10 to 1/1000. The PCR efficiency was calculated using Eq. (1) (Radonić et al. 2004).

$$E\% = 10(1/\text{Slope}) - 1 \times 100. \quad (1)$$

The change in relative mRNA expression of the stemness genes (Botchkina et al. 2010; Rao et al. 2013) *Nanog, Oct4, c-MYC* and *CD133* was assessed using the standard curve method (Larionov et al. 2005). All samples were normalized to GAPDH transcript abundance (TA) as the internal control.

Low-LET irradiation

Irradiation was performed using a clinical accelerator (Neptun 10 PC) at source-to-surface distance (SSD) of 100 cm and a 20×20 cm^2 field size. Mega-voltage radiation (9 MV) was delivered at a total dose of 2, 4, 6 and 8 Gy with a dose rate of 300 cGy min^{-1}. In vivo radiation diode dosimetry measurements were carried out for the beam calibration and the variation within a field was smaller than 2% for each well. After irradiation, cells were incubated at 37 °C, with 5% (v/v) CO_2.

Clonogenic assay

Survival fractions were determined based on colony formation assays. Both CSLCs (3D spheroids) and parental cells were singled out using a pipette and seeded in six-well plates before irradiation. Fifteen days after irradiation, the cells were rinsed with PBS, fixed and stained with a 4% (v/v) paraformaldehyde solution, hematoxylin and eosin stains, respectively. Colonies with more than 50 cells were counted in triplicate with the Image Master 2D platinum software (Buckinghamshire, England). The relative cell surviving fraction was calculated by dividing the number of colonies of treated cells by that of the control (Chen et al. 2010).

Table 1 List of primers

Gene name	5′ → 3′	References
Nanog F	CCCCAGCCTTTACTCTTCCTA	PrimerBank ID:153945815c3
Nanog R	CCAGGTTGAATTGTTCCAGGTC	
Oct4 F	GAGAACCGAGTGAGAGGC AACC	RTPrimerDB ID: 3579
Oct4 R	CATAGTCGCTGCTTGATC GCTTG	
c-MYC F	GGCTCCTGGCAAAAGGTCA	PrimerBank ID: 239582723c1
c-MYC R	CTGCGTAGTTGTGCTGATGT	
CD133 F	AGAGCTTGCACCAACAAAGTA CAC	RTPrimerDB ID: 691
CD133 R	AAGCACAGAGGGTCATTG AGAGA	
GAPDH F	ACAACTTTGGTATCGTGGAAGG	PrimerBank ID: 378404907c2
GAPDH R	GCCATCACGCCACAGTTTC	

Radioresistance analysis

Radiobiological parameters

For a single acute dose, a radiation survival curve was drawn using the LQ-model (Weichselbaum et al. 1990) (Eq. 2) and the area under the survival curve was calculated using Eq. (3), which represents the mean inactivation dose (Fertil et al. 2012) (MID):

$$S = \exp\left(-(\alpha D + \beta D^2)\right) \quad (2)$$

$$\text{MID} = \int S(D)\text{d}(D). \quad (3)$$

The sensitivity enhancement ratio (SER) value and the RBE value at D_{10} (dose required to reduce the survival fraction to 10%) were calculated according to the following equations (Jain et al. 2011; Hirota et al. 2014; Takahashi et al. 2014b):

$$\text{SER} = \text{MID (X-ray)}/\text{MID (X-ray + GNPs)} \quad (4)$$

$$\text{RBE} = D_{10}(\text{X-ray})/D_{10}(\text{X-ray + GNPs}). \quad (5)$$

The radiobiological parameters α and β were estimated based on LQ model. Also, multi-target single hit model (Weichselbaum et al. 1990) (Eq. 6) was used to extract the shoulder of the survival curve (Hall and Willson 1988; Bodgi et al. 2016) (n) and the mean lethal dose (Halperin et al. 2007; Hall and Willson 1988) (D_0).

$$S = 1 - \left(1 - e^{-D/D_0}\right)^n. \quad (6)$$

Cell cycle analyses

Cells were trypsinized and washed twice in PBS, then 10^6 cells were fixed overnight in 70% (v/v) ethanol at −20 °C. The cells were centrifuged, resuspended in 0.5 mL of a propidium iodide (PI) staining solution (containing 50 μg mL^{-1} PI and 10 μg mL^{-1} RNase) for 30 min at RT. Samples were analyzed using a FACS Calibur flow cytometer (BD Biosciences, San Jose, CAUSA). Cell cycle distribution was evaluated before irradiation and 24 h after exposure to 2 and 6 Gy irradiation doses.

ϒ-H2AX detection by immunofluorescence

Phosphorylation of histone H2AX is a quantitative biomarker for the identification of DNA double-strand breaks (DSBs) in cells (Ismail et al. 2007). HT29 CSLCs and parental cells were seeded into six-well tissue culture plates containing a sterilized cover glass and irradiated with 4 Gy dose of X-rays in the presence and absence of GNPs. Cultures were fixed for 20 min with fresh 4% (v/v) paraformaldehyde and permeabilized with 0.1% (v/v) Triton X-100, 2 and 24 h after irradiation. Cells were blocked with 5% (w/v) BSA in PBS for 40 min at room temperature. The samples were incubated with anti-phospho-histone H2AX (Ser139, clone JBW301) mouse monoclonal IgG1 (Upstate) overnight at 4 °C and followed by secondary antibodies Alexa Fluor1 488 donkey anti-mouse IgG (H + L) for 45 min at room temperature. The cell nuclei were stained with 4′,6-diamidino-2-phenylindole (DAPI) for 10 min. The cover slips were mounted on microscope slides using Vectashield antifade (Vector Laboratories, Burlingame, CA) and examined with a fluorescence microscope (Olympus, magnification: 100 × objective). The number of ϒ-H2AX foci were counted in 25 nuclei, at least.

Statistical analysis

Differences between irradiated groups with GNPs and without GNPs were analyzed with the paired Student's *t* test in each cell population. The independent Student's *t* tests were performed to analyze the difference between two different cell populations. Differences less than 0.05 (P value < 0.05) were considered statistically significant and values are presented as mean ± SD. All experiments were performed in triplicate and repeated at least three times.

Results

Serum-free medium upregulated expression of stemness genes and formed spheroid-like structures in HT29 colorectal cancer cells

Evidently, differentiated carcinoma cells died a few days after incubation in a serum-free culture medium (SFM). However, the cells with stem cell features survived and grew as spheroid-like structures (Wei et al. 2012). As shown in Fig. 1, sphere formation started on the third day and they reached maximum size after 10 days on collagen type I-coated plate in SMF (Col/SFM). After approximately 10 days of culture, the spheres emerged like a ball, round with a smooth surface. Also, SEM images showed that they had a vaulted structure in Col/SFM (Fig. 2).

Flow cytometry analyses indicated that the proportion of CD133, as a specific surface marker for colorectal CSLCs (Wei et al. 2012), in parental HT29 cells was approximately 35%. However, in Col/SFM the percentage of CD133 in HT29 CSLCs was dramatically increased to 72% as shown in Fig. 3a.

In qRT-PCR analysis, the transcript abundances (TAs) of the stemness genes *Nanog, Oct4, c-MYC* and *CD133* were higher in the HT29 CSLCs compared with the parental cells (P value < 0.05) (Fig. 3b).

Cell cycle progression differs in HT29 CSLCs and parental cells

Cell cycle distribution is one of the intrinsic factors that affect the degree of radiosensitization. As displayed in Fig. 4a, HT29 CSLCs had a significantly higher proportion of G_0/G_1 phase cells compared with parental cells (P value < 0.05), whereas the G_2/M phase proportion was significantly lower (P value < 0.05). This result indicated that the HT29 CSLC population are in a quiescence state and, as a result, may be more radioresistant than their parental cells (Moore and Lyle 2011; Sun and Cabarcas 2012).

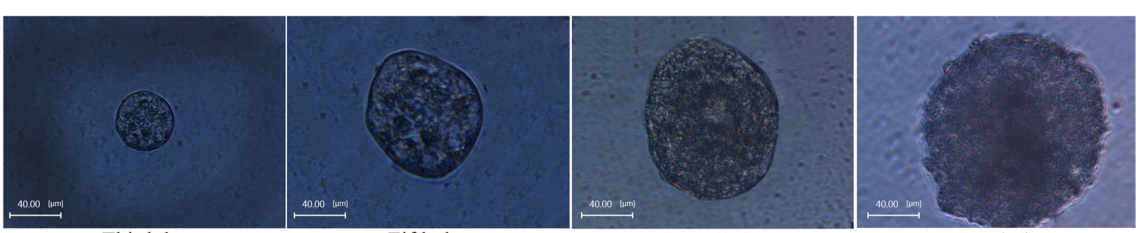

Fig. 1 Inverted optical microscopy showed the growth of spheroid-like structures that formed in Col/SFM (magnification: × 40 objective)

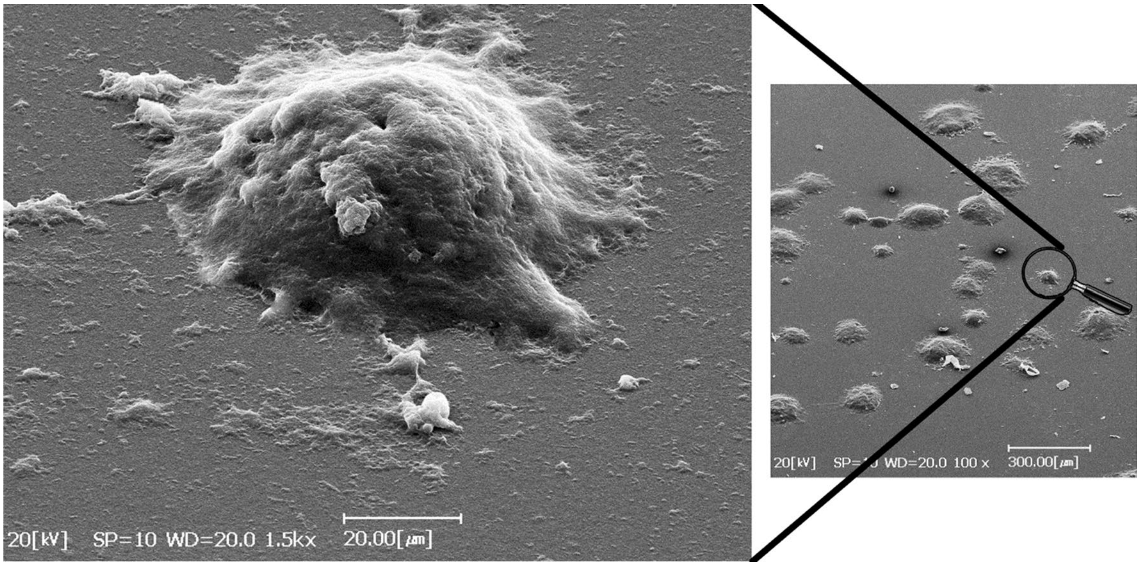

Fig. 2 SEM images of HT29 spheroid-like structures after 10 days of culture in Col/SFM

Radiation remarkably redistributes HT29 parental cell cycle but has less effect on CSLCs

Activation of cell cycle checkpoint is one of the mechanisms of DNA damage repair (Wiskirchen et al. 2001). Figure 4a shows the cell cycle distribution for HT29 CSLCs and parental cells 48 h after 2 Gy and 6 Gy irradiation. These results indicated that in parental cells a dose-dependent cell cycle delay at the G_2/M phase was accompanied by a proportional decrease of cells in G_0/G_1 phase. By contrast, less prominent G_2 phase retardation was displayed in HT29 CSLCs at different radiation doses. Therefore, the effects of radiation, such as cell cycle arrest on HT29 CSLCs, were significantly weaker than those on parental cells. Moreover, irradiation did not induce significant changes in the cell cycle phase distribution of HT29 CSLCs compared with parental cells (Fig. 4b, c).

Radiation in the presence of GNPs decreases the radioresistance of HT29 CSLCs

The radiosensitivity of HT29 CSLCs and parental cells in presence and absence of GNPs was analyzed using clonogenic assays. Cell survival curves and related radiobiological parameters are presented in Fig. 5 and Table 2. Compared with parental cells, HT29 CSLCs showed higher survival following irradiation over a wide dose range (P value < 0.05).

The survival fraction of the HT29 CSLCs and parental cells at 2 Gy was 92% and 75%, respectively (P value < 0.05). The shoulder of the HT29 CSLC survival curve (n) was wider than that of the parental cells. The radiobiological parameters MID (mean inactivation dose) and D_0 (mean lethal dose) in the HT29 CSLCs were significantly higher than those observed in parental cells (P value < 0.05) which suggests more radiosensitivity of parental cells. Also, the linear components of survival curves (α) were significantly smaller in HT29 CSLCs than in parental cells.

The survival fraction of the HT29 CSLCs and parental cells in the presence of GNPs significantly decreased compared with irradiation alone. The SER value of HT29 CSLCs and parental cells were 1.8 and 1.4, respectively. Changes in the linear component and shoulder of the survival curve in the presence of GNPs were evaluated. These parameters determine the type of irradiation-induced cell death and highlight the difference between high and low LET (Hall and Willson). Surprisingly, in the presence of GNPs, the linear component of the survival curve for HT29 CSLCs significantly increased and the shoulder decreased, as expected for high LET (P value < 0.05) (Hall and Willson). We found that the RBE values for HT29 CSLCs and parental cells (for X-ray + GNP beam relative to X-ray alone at D_{10} level) were about 1.6 and 1.27, respectively.

Induction and persistence of DNA-DSBs in the presence of GNPs were increased in both HT-29 CSLCs and parental cells

DNA DSBs were investigated by ϒ-H2AX assays following 4 Gy X-ray irradiation of HT29 CSLCs and parental cells. As shown in Fig. 6, in parental cells, the number of foci induced after 2 h was significantly higher than those induced in CSLCs (P value < 0.05). These results indicate

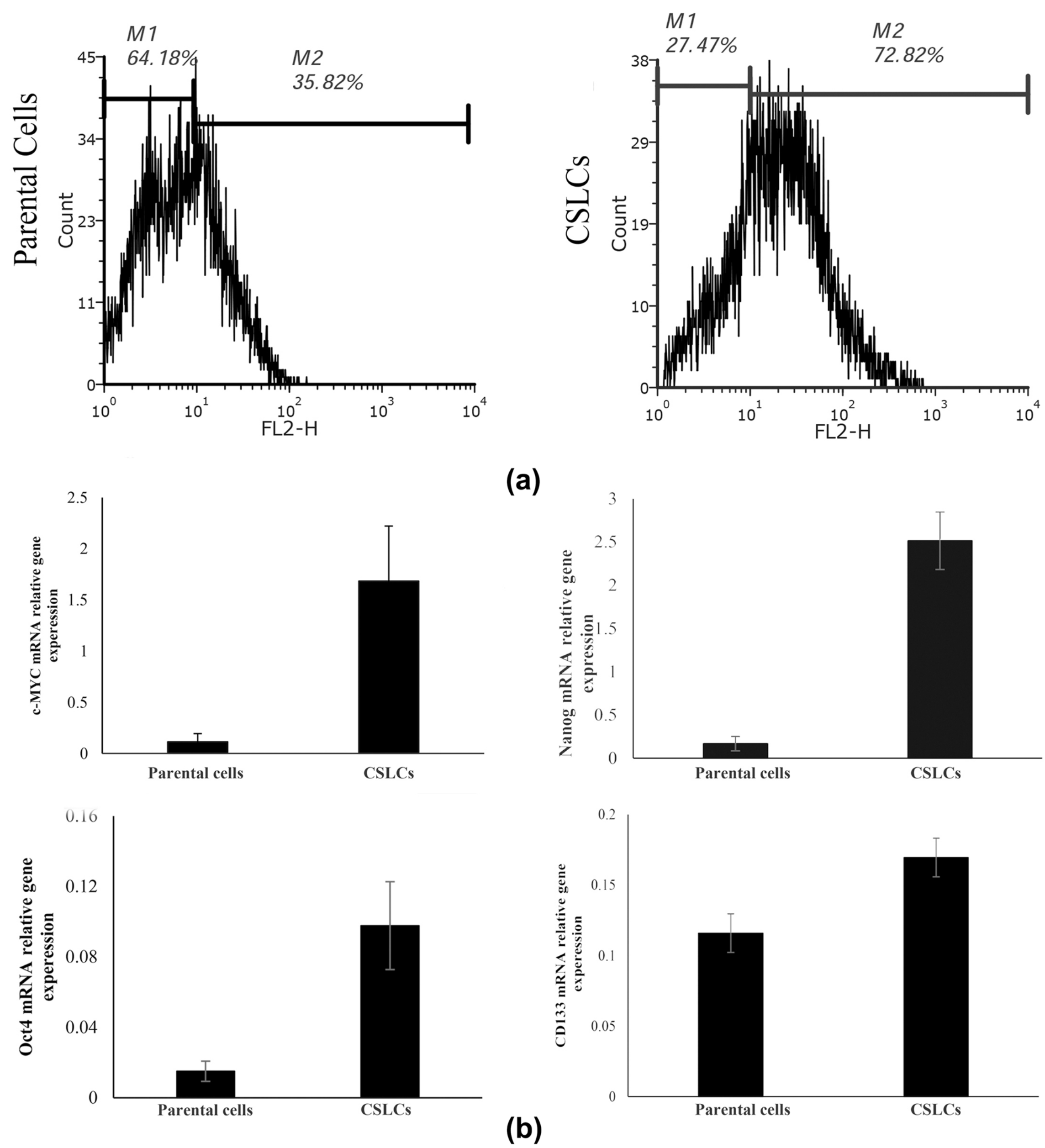

Fig. 3 **a** Expression level of the CD133 surface marker and **b** transcript abundances of stemness genes in HT29 CSLCs and parental cells

that parental cells were more susceptible to DNA DSBs. In addition, the number of persistent ϒ-H2AX foci 24 h after irradiation and unrepairable DNA DSBs in HT-29 CSLCs was lower than parental cells (*P* value < 0.05). Compared to radiation alone in the presence of GNPs, the numbers of ϒ-H2AX foci induced 2 and 24 h after irradiation in both HT29 CSLCs and parental cells were significantly increased (*P* value < 0.05).

Discussion

Recent studies reported that a sub-population of solid tumors (CSLCs) was highly resistant to conventional radiation therapies (Nguyen et al. 2011; Cui et al. 2011; Moncharmont et al. 2012). Thus, the purpose of this study was to evaluate the radiosensitization enhancement of CSLCs in the third most common malignancy, colorectal cancer (Siegel et al. 2014), in the presence of GNPs and low-LET irradiation (X-ray). To approach this goal, we used HT29, the most radioresistant colorectal cancer cell

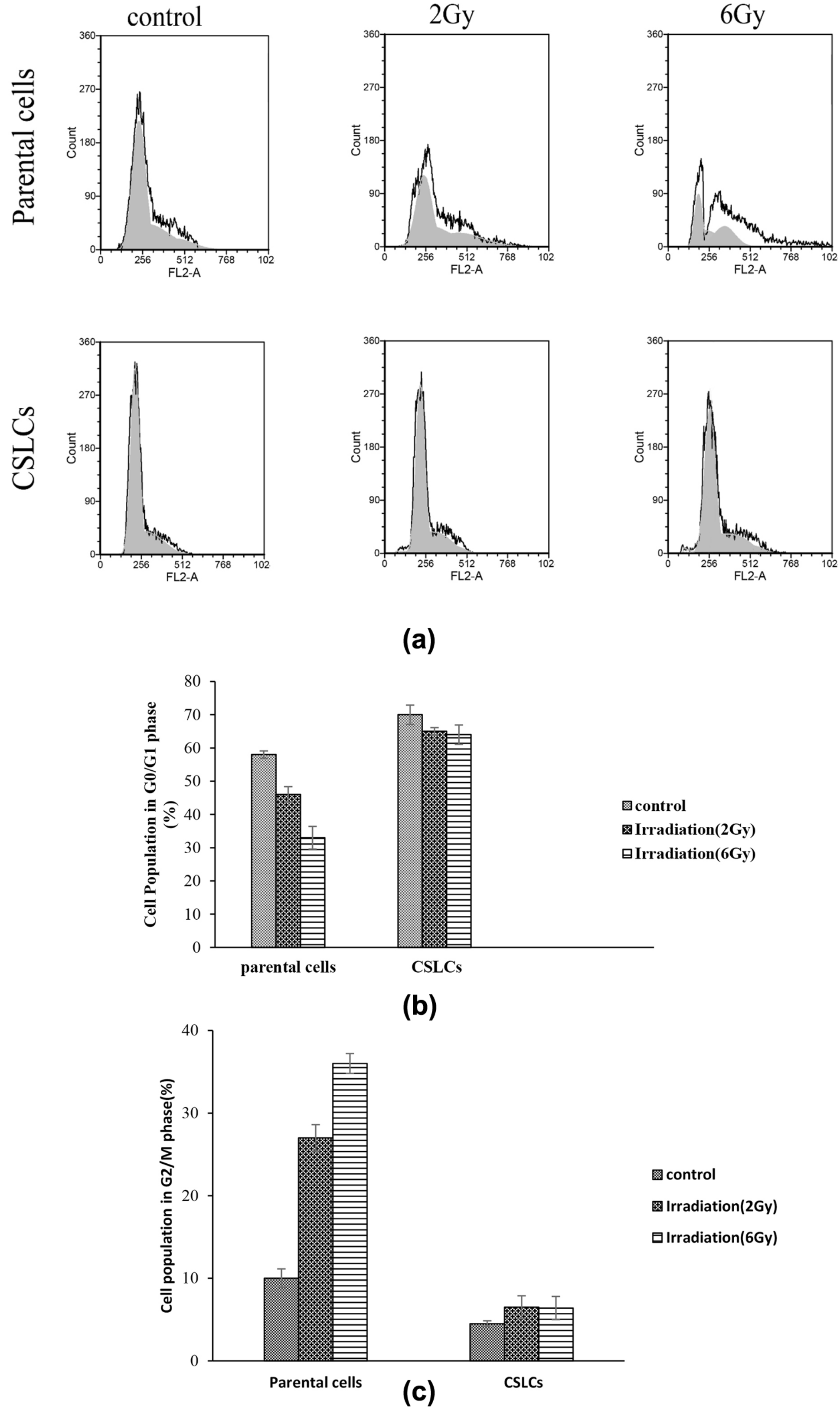

Fig. 4 Cell cycle analysis of HT29 CSLCs and parental cells before and after irradiation with different radiation doses. **a** Distribution of cell populations to different cell cycle phases was analyzed using flow cytometry analysis. **b** The proportion of G_0/G_1 population. **c** The proportion of G_2/M population

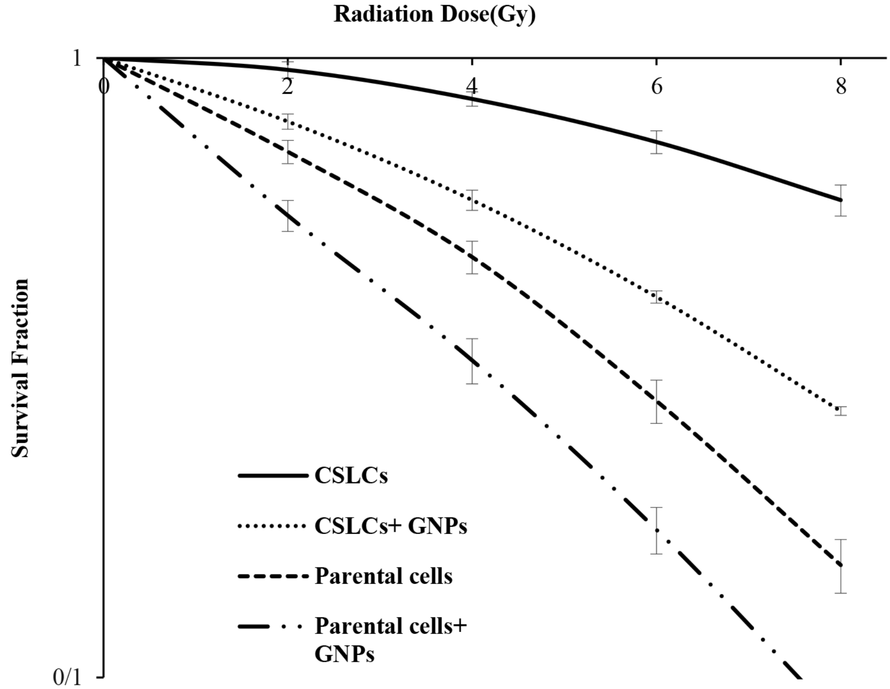

Fig. 5 The dose–response curves of HT29 CSLCs and parental cells in the presence and absence of GNPs

Table 2 Radiobiological parameters of HT29 CSLCs and parental cells after irradiation

Parameters	Parental cells	CSLCs	Parental cells + GNPs	CSLCs + GNPs
SF_2[a]	75%	92%	56%	78%
α	0.14	0.03	0.25	0.1
MID	5.02	10.39	3.61	5.8
n	1.6	2.2	1.1	1.8
D_0	3.4	5.1	3.2	4.5
D_{50}[b]	4.29	10	2.68	5
SER	–	–	1.4	1.8
RBE	–	–	1.27	1.6

[a]Survival fraction at 2 Gy

[b]The irradiation dose that kills half of the cells

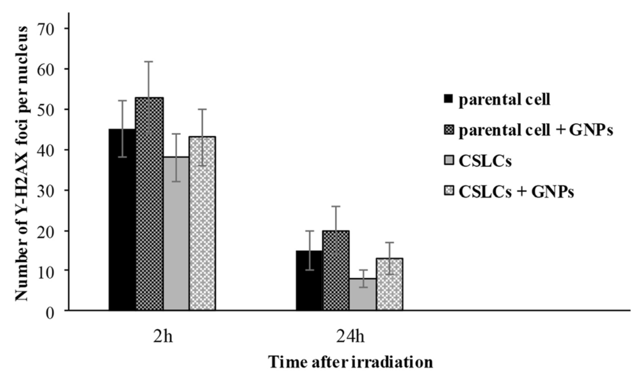

Fig. 6 The number of ϒ-H2AX foci in HT29 CSLCs and parental cells after 4 Gy irradiation in the presence and absence of GNPs

line (Frykholm et al. 1991; Dunne et al. 2003). The HT29 CSLCs were isolated, characterized, and the intrinsic radioresistance properties evaluated. Spheroid-like structures in Col/SFM expressed the CD133 surface marker by 72%. Similarly, the TAs of the stemness-related genes *CD133, Oct4, c-MYC* and *Nanog* were relatively high. These results were consistent with previous reports that used the SFM medium for CSLC enrichment (Kirkland 2009; Fang et al. 2010; Wei et al. 2012).

The intrinsic radioresponsiveness of HT29 CSLCs was assessed by plotting a clonogenic survival curve. As shown in previous studies (Parfitt et al. 2011; Martins-Neves et al. 2012), low values of linear components (α) of survival curves indicate high intrinsic radioresistance, low induced lethal damage and low apoptosis stimuli. Therefore, the intrinsic radioresistance of HT29 CSLCs was expected to be higher than parental cells because of their lower α value (see Fig. 5; Table 2). Similarly, a high value of the survival curve shoulder (n) observed in HT29 CSLCs suggested high rates of repair of both sublethal and potentially lethal damage, as previously reported (Phillips et al. 2006; Martins-Neves et al. 2012). Consistently, the ϒ-H2AX assay showed less susceptibility to DNA DSB induction in HT29 CSLCs than parental cells 2 h after irradiation, thus suggesting high radioresistance for HT29 CSLCs (Diehn et al. 2009; Jamal et al. 2012). Unrepairable DNA DSBs were determined 24 h after irradiation by counting the number of persisting

ϒ-H2AX foci (Schmid et al. 2010; Hirota et al. 2014). The much faster rate of reduction of foci number in HT29 CSLCs indicated a larger DSBs restoration capacity than parental cells (Taneja et al. 2004; Menegakis et al. 2009; Oonishi et al. 2012; Hirota et al. 2014). Therefore, more complex DNA DSBs such as those occurred in high-LET irradiation are needed for HT29 CSLC eradication. Furthermore, the cell cycle distribution before and after irradiation, as a key parameter of intrinsic radioresponsiveness (Kim et al. 2012), was investigated. Before irradiation, HT29 CSLCs had higher G_0/G_1 and lower G_2/M phase ratios compared to their parental cells. This may indicate that they are relatively quiescent and have a slow cycling rate as was previously reported for CSLCs (Martins-Neves et al. 2012; Lundholm et al. 2013). The quiescent state results in an intrinsic defense mechanism that enables CSLCs to be resistant to therapeutic approaches that target rapidly dividing cells (Diaz and Leon 2011). Forty-eight hours after irradiation, there was no obvious change in the cell cycle distribution of HT29 CSLCs. However, the population of cells in G_2 phase was significantly increased in parental cells (Fig. 4). The remarkable ability to repair irradiation damage may enable CSLCs to pass checkpoint arrests more rapidly than parental cells (Eyler and Rich 2009). Consequently, in line with previous reports (Martins-Neves et al. 2012; Lundholm et al. 2013), the results here suggest that alterations in the checkpoint responses might allow HT29 CSLCs to circumvent the pro-apoptotic effects of radiation therapy and, therefore, cause both a decrease in cell death and an increase in cell proliferation activity.

Intrinsic CSLC properties, such as propensity for quiescence, enhanced DNA repair, unregulated cell cycle control systems and free radical scavenging mechanisms, may enable them to tolerate the effects of treatments such as low-LET irradiation. In low-LET irradiation, the production of free radicals causes both sub-lethal and potentially lethal damage (Phillips et al. 2006; Escherichia and Billen 2014). Controversially, a direct action with high-LET irradiation predominantly induced clustered unrepairable DNA damages that finally increased RBE and decreased cell cycle-dependent radiosensitivity (Hada and Georgakilas 2008; Okayasu 2012). Here, the combination of GNPs with X-ray energy enhanced radiosensitization of HT29 CSLCs. The internalized GNPs significantly increased the α and decreased the n components of survival curves, probably because of an increased absorbed dose. Additionally, unrepairable DNA DSBs in CSLCs were significantly increased in the presence of GNPs. These results may be consistent with the expected high-LET irradiation effects (Hall and Willson 1988; Suzuki et al. 2000; Hirota et al. 2014). While there is some evidence that lethal effects of Auger electrons may exist if the GNPs are localized intracellularly, more lethal damage can occur when the Auger electrons are generated at a position closer to the DNA (nucleus) (Chithrani et al. 2010; Xu et al. 2012; Chattopadhyay et al. 2013). Although the internalized GNPs might randomly penetrate the nucleus or other cell organelles, we could not ascertain the exact location of the GNPs in the cells (Saberi et al. 2016).

The most striking characteristic that distinguished high-LET radiation from low-LET radiation was the induction of more serious DNA DSBs (Goodhead 1994, 1999). The colony assays of HT29 parental cells showed the RBE values of 1.27 in vitro at D_{10} for X-ray + GNPs (Table 2). In previous studies (Suzuki et al. 2000; Matsui et al. 2004) that used HIMAC carbon-ion beams on different cancer cell lines such as brain, pancreas and lung tumors, the RBE values of 1.06–1.33 for a 13-keV/mm beam were reported. Furthermore, the RBE values of HCT116 and Sw480 colorectal cancer cell lines for a SOBP carbon ion beam were reported as 1.63 and 1.74 for a 50-keV/mm beam, respectively (Cui et al. 2011). The calculated RBE value induced by GNPs + X-ray may be consistent with the range of 13-keV/mm-beam carbon ion. Additionally, the RBE value calculated at the D_{10} level for HT29 CSLCs was about 1.6, significantly higher than parental cells. Theoretically, these findings can be explained by new nanodosimetric models (McMahon et al. 2011a, b; Gadoue et al. 2017). In the presence of GNPs, production of Auger electrons with low energy and a small range resulted in highly non-homogenous dose distributions on the nanoscale. Therefore, in parallel with previous studies that targeted CSLCs with heavy ions (Cui et al. 2011; Hirota et al. 2014; Takahashi et al. 2014b; Sai et al. 2015), it may be implied that the GNPs plus X-ray induced more complex DNA damages compared to X-rays alone, possibly due to the higher RBE value of HT29 CSLCs than parental cells. Moreover, these results suggest that this combination has a promising potential to destroy HT29 cancer stem-like cells.

The results indicated that the GNPs + X-ray treatment has advantages over X-rays to eradicate HT29 CSLCs. Thus, this method can be considered as an alternative for high-LET irradiation. It is important, however, to consider that the radiosensitization enhancement shown in this study may not necessarily translate directly to a clinical outcome that may depend on in vivo biological and physiological conditions. In the next step, we aim to conjugate the GNPs with ligands (Tazi et al. 2011; Li and Howell 2010; van der Meel et al. 2012; Wang et al. 2012; Mahon et al. 2012; Ning et al. 2016) that enable them to selectively target in vivo the putative colorectal CSLC surface markers such as CD133, CD44, CD90 and EpCAM (Fanali 2014).

Acknowledgements The authors are highly thankful to all technicians who provided support during the course of research. The part of this work was supported by Stem Cell Research Center, Golestan University of Medical Science (Grant no: 950818185).

Author contributions ABZ and AM designed the research. ABZ, AM and BA performed the experiments. ABZ, AM, and LDA contributed to analysis and interpretation of data. AM and ABZ wrote the manuscript. All authors reviewed the manuscript.

Compliance with ethical standards

Conflict of interest The author(s) declare no competing interests.

Ethical approval This article does not contain any studies with human participants or animals performed by any of the authors.

References

Arab-Bafrani Z, Shahbazi-Gahrouei D, Abbasian M et al (2016) Multiple MTS assay as the alternative method to determine survival fraction of the irradiated HT-29 colon cancer cells. J Med Signals Sens 6:112–116

Bodgi L, Canet A, Pujo-Menjouet L et al (2016) Mathematical models of radiation action on living cells: from the target theory to the modern approaches. A historical and critical review. J Theor Biol 394:93–101

Botchkina GI, Zuniga ES, Das MM et al (2010) New-generation taxoid SB-T-1214 inhibits stem cell-related gene expression in 3D cancer spheroids induced by purified colon tumor-initiating cells. Mol Cancer 9:1–12

Butterworth KT, Coulter JA, Jain S et al (2011) Evaluation of cytotoxicity and radiation enhancement using 1.9 nm gold particles: potential application for cancer therapy. Nanotechnology 21(29):295101

Chattopadhyay N, Cai Z, Kwon YL et al (2013) Molecularly targeted gold nanoparticles enhance the radiation response of breast cancer cells and tumor xenografts to X-radiation. Breast Cancer Res Treat 137:81–91

Chen W-S, Lee Y-J, Yu Y-C et al (2010) Enhancement of p53-mutant human colorectal cancer cells radiosensitivity by flavonoid fisetin. Int J Radiat Oncol Biol Phys 77:1527–1535

Chithrani DB, Jelveh S, Jalali F et al (2010) Gold nanoparticles as radiation sensitizers in cancer therapy. Radiat Res 173:719–728

Cui X, Oonishi K, Tsujii H et al (2011) Effects of carbon ion beam on putative colon cancer stem cells and its comparison with X-rays. Cancer Res 71:3676–3687

Diaz A, Leon K (2011) Therapeutic approaches to target cancer stem cells. Cancers (Basel) 3:3331–3352

Diehn M, Cho RW, Lobo NA et al (2009) Association of reactive oxygen species levels and radioresistance in cancer stem cells. Nature 458:780–783

Dunne AL, Price ME, Mothersill C et al (2003) Relationship between clonogenic radiosensitivity, radiation-induced apoptosis and DNA damage/repair in human colon cancer cells. Br J Cancer 89:2277–2283

Escherichia R, Billen D (2014) Free radical scavenging and the expression of potentially lethal damage in X-irradiated repair-deficient *Escherichia coli*. Radiat Res 111:354–360

Eyler CE, Rich JN (2009) Survival of the fittest: cancer stem cells in therapeutic resistance and angiogenesis. J Clin Oncol 26:2839–2845

Fanali C (2014) Cancer stem cells in colorectal cancer from pathogenesis to therapy: controversies and perspectives. World J Gastroenterol 20:923

Fang DD, Kim YJ, Lee CN et al (2010) Expansion of CD133(+) colon cancer cultures retaining stem cell properties to enable cancer stem cell target discovery. Br J Cancer 102:1265–1275

Fertil B, Dertinger H, Courdi A, Malaise EP (2012) Mean inactivation dose: a useful concept for intercomparison of human cell survival curves. Radiat Res 178:AV237–AV243

Frykholm G, Glimelius B, Richter S, Carlsson J (1991) Heterogeneity in antigenic expression and radiosensitivity in human colon carcinoma cell lines. In Vitro Cell Dev Biol 27A:900–906

Gadoue SM, Toomeh D, Zygmanski P, Sajo E (2017) Angular dose anisotropy around gold nanoparticles exposed to X-rays. Nanomed Nanotechnol Biol Med 13:1653–1661

Gandomani HS, Yousefi SM, Aghajani M et al (2017) Colorectal cancer in the world: incidence, mortality and risk factors. Biomed Res Ther 4:1656

Garza-Treviño EN, Said-Fernández SL, Martínez-Rodríguez HG (2015) Understanding the colon cancer stem cells and perspectives on treatment. Cancer Cell Int 15:2

Girard YK, Wang C, Ravi S et al (2013) A 3D fibrous scaffold inducing tumoroids: a platform for anticancer drug development. PLoS One 8:e75345

Goodhead DT (1994) Initial events in the cellular effects of ionizing radiations: clustered damage in DNA. Int J Radiat Biol 65:7

Goodhead DT (1999) Mechanisms for the biological effectiveness of high-LET radiations. J Radiat Res 40(Suppl):1–13

Hada M, Georgakilas AG (2008) Formation of clustered DNA damage after high-LET irradiation: a review. J Radiat Res 49:203–210

Hall EJ, Willson S (1988) Radiobiology for the radiologist. Wolters Kluwer, Philadelphia

Halperin EC, Perez CA, Brady LW (2007) Principles and practice of radiation oncology. Wolters-Kluwer, Philadelphia

He Z, Subramaniam D, Zhang Z et al (2009) Honokiol radiosensitizes colorectal cancer cells: enhanced activity in cells with mismatch repair defects. AJP Gastrointest Liver Physiol 301:G929–G937

Held KD, Kawamura H, Kaminuma T et al (2016) Effects of charged particles on human tumor cells. Front Oncol 6:23

Hirota Y, Masunaga SI, Kondo N et al (2014) High linear-energy-transfer radiation can overcome radioresistance of glioma stem-like cells to low linear-energy-transfer radiation. J Radiat Res 55:75–83

Ismail IH, Wadhra TI, Hammarsten O (2007) An optimized method for detecting gamma-H2AX in blood cells reveals a significant interindividual variation in the gamma-H2AX response among humans. Nucleic Acids Res 35:e36

Jain S, Ch B, Coulter JA, Hounsell ARKT (2011) Cell-specific radiosensitization by gold nanoparticles at megavoltage radiation energies. Int J Radiat Oncol Biol Phys 79:531–539

Jamal M, Rath BH, Tsang PS et al (2012) The brain microenvironment preferentially enhances the. Neoplasia 14:150–158

Kahlert UD, Mooney SM, Natsumeda M et al (2017) Targeting cancer stem-like cells in glioblastoma and colorectal cancer through metabolic pathways. Int J Cancer 140:10–22

Khiari H, Hsairi M (2017) Colorectal cancer incidence and clinicopathological features in northern Tunisia 2007–2009. Color Cancer 6:131–141

Kim S, Rhee JG, Song X et al (2012) Breast cancer stem cell-like cells are more sensitive to ionizing radiation than non-stem cells: role of ATM. PLoS One 7:e50423

Kirkland SC (2009) Type I collagen inhibits differentiation and promotes a stem cell-like phenotype in human colorectal carcinoma cells. Br J Cancer 101:320–326

Larionov A, Krause A, Miller W (2005) A standard curve based method for relative real time PCR data processing. BMC Bioinform 6:62

Li S-D, Howell SB (2010) CD44-targeted microparticles for delivery of cisplatin to peritoneal metastases. Mol Pharm 7:280–290

Liu Z, Xiong L, Ouyang G et al (2017) Investigation of copper cysteamine nanoparticles as a new type of radiosensitizers for colorectal carcinoma treatment. Sci Rep 7:1–11

Lundholm L, Hååg P, Zong D, Juntti T, Mörk B, Lewensohn RVK (2013) Resistance to DNA-damaging treatment in non-small cell lung cancer tumor-initiating cells involves reduced DNA-PK/ATM activation and diminished cell cycle arrest. Cell Death Dis 4:e478

Mahon E, Salvati A, Baldelli Bombelli F et al (2012) Designing the nanoparticle-biomolecule interface for "targeting and therapeutic delivery". J Control Release 161:164–174

Martins-Neves SR, Lopes ÁO, Carmo A et al (2012) Therapeutic implications of an enriched cancer stem-like cell population in a human osteosarcoma cell line. BMC Cancer 12:139

Matsui Y, Asano T, Kenmochi T et al (2004) Effects of carbon-ion beams on human pancreatic cancer cell lines that differ in genetic status. Am J Clin Oncol 27:24–28

McMahon SJ, Hyland WB, Muir MF et al (2011a) Biological consequences of nanoscale energy deposition near irradiated heavy atom nanoparticles. Sci Rep 1:18

McMahon SJ, Hyland WB, Muir MF et al (2011b) Nanodosimetric effects of gold nanoparticles in megavoltage radiation therapy. Radiother Oncol 100:412–416

Menegakis A, Yaromina A, Eicheler W et al (2009) Prediction of clonogenic cell survival curves based on the number of residual DNA double strand breaks measured by γH2AX staining. Int J Radiat Biol 85:1032–1041

Moncharmont C, Levy A, Gilormini M et al (2012) Targeting a cornerstone of radiation resistance: cancer stem cell. Cancer Lett 322:139–147

Moore N, Lyle S (2011) Quiescent, slow-cycling stem cell populations in cancer: a review of the evidence and discussion of significance. J Oncol 2011:396076

Nguyen GH, Murph MM, Chang JY (2011) Cancer stem cell radioresistance and enrichment: where frontline radiation therapy may fail in lung and esophageal cancers. Cancers (Basel) 3:1232–1252

Niemantsverdriet M, Goethem Van M et al (2012) High and low LET radiation differentially induce normal tissue damage signals. Radiat Oncol Biol 83:1291–1297

Ning S-T, Lee S-Y, Wei M-F et al (2016) Targeting colorectal cancer stem-like cells with anti-CD133 antibody-conjugated SN-38 nanoparticles. ACS Appl Mater Interfaces 8:17793–17804

Okayasu R (2012) Repair of DNA damage induced by accelerated heavy ions—a mini review. Int J Cancer 130:991–1000

Okayasu R, Okada M, Okabe A et al (2006) Repair of DNA damage induced by accelerated heavy ions in mammalian cells proficient and deficient in the non-homologous end-joining pathway. Radiat Res 165:59–67

Oonishi K, Cui X, Hirakawa H et al (2012) Different effects of carbon ion beams and X-rays on clonogenic survival and DNA repair in human pancreatic cancer stem-like cells. Radiother Oncol 105:258–265

Parfitt SL, Milner RJ, Salute ME et al (2011) Radiosensitivity and capacity for radiation-induced sublethal damage repair of canine transitional cell carcinoma (TCC) cell lines. Vet Comp Oncol 9:232–240

Phillips TM, Mcbride WH, Pajonk F (2006) The response of CD24 −/low/CD44 + breast cancer—initiating cells to radiation. J Natl Cancer Inst 98:1777–1785

Radonić A, Thulke S, Mackay IM et al (2004) Guideline to reference gene selection for quantitative real-time PCR. Biochem Biophys Res Commun 313:856–862

Rao G, Liu H, Li B et al (2013) Establishment of a human colorectal cancer cell line P6C with stem cell properties and resistance to chemotherapeutic drugs. Acta Pharmacol Sin 34:793–804

Roy S, Majumdar AP (2012) Signaling in colon cancer stem cells. J Mol Signal 7:11

Saberi A, Shahbazi-Gahrouei D, Abbasian M et al (2016) Gold nanoparticles in combination with megavoltage radiation energy increased radiosensitization and apoptosis in colon cancer HT-29 cells. Int J Radiat Biol 93:315–323

Sai S, Vares G, Kim EH et al (2015) Carbon ion beam combined with cisplatin effectively disrupts triple negative breast cancer stem-like cells in vitro. Mol Cancer 14:166

Schmid TE, Dollinger G, Beisker W et al (2010) Differences in the kinetics of γ-H2AX fluorescence decay after exposure to low and high LET radiation. Int J Radiat Biol 86:682–691

Siegel R, DeSantis C, Jemal A (2014) Colorectal cancer statistics, 2014. CA Cancer J Clin 64:104–117

Sun L, Cabarcas SM (2012) Radioresistance and cancer stem cells: survival of the fittest. J Carcinog Mutagen 1:1–12

Suzuki M, Kase Y, Yamaguchi H et al (2000) Relative biological effectiveness for cell-killing effect on various human cell lines irradiated with heavy-ion medical accelerator in Chiba (HIMAC) carbon-ion beams. Int J Radiat Oncol 48:241–250

Takahashi A, Ma H, Nakagawa A et al (2014a) Carbon-ion beams efficiently induce cell killing in X-ray resistant human squamous tongue cancer cells. IJMPCERO 3:133–142

Takahashi M, Hirakawa H, Yajima H et al (2014b) Carbon ion beam is more effective to induce cell death in sphere-type A172 human glioblastoma cells compared with X-rays. Int J Radiat Biol 90:1125–1132

Taneja N, Davis M, Choy JS et al (2004) Histone H2AX phosphorylation as a predictor of radiosensitivity and target for radiotherapy. J Biol Chem 279:2273–2280

Tazi I, Nafil H, Mahmal L (2011) Monoclonal antibodies in hematological malignancies: past, present and future. J Cancer Res Ther 7:399–407

van der Meel R, Oliveira S, Altintas I et al (2012) Tumor-targeted nanobullets: anti-EGFR nanobody-liposomes loaded with anti-IGF-1R kinase inhibitor for cancer treatment. J Control Release 159:281–289

Wang L, Su W, Liu Z et al (2012) CD44 antibody-targeted liposomal nanoparticles for molecular imaging and therapy of hepatocellular carcinoma. Biomaterials 33:5107–5114

Wei B, Han X-Y, Qi C-L et al (2012) Coaction of spheroid-derived stem-like cells and endothelial progenitor cells promotes development of colon cancer. PLoS One 7:e39069

Weichselbaum RR, Beckett MA, Vijayakumar S et al (1990) Radiobiological characterization of head and neck and sarcoma cells derived from patients prior to radiotherapy. Int J Radiat Oncol Biol Phys 19:313–319

Wiskirchen J, Dittmann H, Kehlbach R et al (2001) Rhenium-188 for inhibition of human aortic smooth muscle cell proliferation. Int J Radiat Oncol Biol Phys 49:809–815

Xu W, Luo T, Pang B et al (2012) The radiosensitization of melanoma cells by gold nanorods irradiated with MV X-ray. Nano Biomed Eng 4:6–11

Yan C, Luo L, Goto S et al (2016) Enhanced autophagy in colorectal cancer stem cells does not contribute to radio-resistance. Oncotarget 7:45112